

Supporting Information

Naphthalimide End Capped Anthraquinone Based Solution-Processable *n*-Channel Organic Semiconductors: Effect of Alkyl Chain Engineering on Charge Transport

Thu-Trang Do,^a Yasunori Takeda,^b Sergei Manzhos,^c John Bell,^a Shizuo Tokito^{b} and Prashant*

Sonar^{a}*

^aSchool of Chemistry, Physics and Mechanical Engineering, Queensland University of Technology (QUT), 2 George Street, Brisbane, QLD-4001, Australia.

^bResearch Center for Organic Electronics, Yamagata University, 4-3-16 Jonan, Yonezawa, Yamagata, 992-8510, Japan.

^cDepartment of Mechanical Engineering, Faculty of Engineering, National University of Singapore

Corresponding email: sonar.prashant@qut.edu.au

Keywords: 1,8-Naphthalimide, 9,10-Anthraquinone, Branched Alkyl Chain, Organic Semiconductors, Field Effect Transistors.

Contents

1. Figure S1. (a) ^1H NMR (400 MHz, CDCl_3) spectrum and (b) ^{13}C NMR (100 MHz, CDCl_3) spectrum of **NAI-ANQ-NAI (BO)**
2. Figure S2. (a) ^1H NMR (400 MHz, CDCl_3) spectrum and (b) ^{13}C NMR (100 MHz, CDCl_3) spectrum of **NAI-ANQ-NAI (HD)**
3. Figure S3. (a) ^1H NMR (400 MHz, CDCl_3) spectrum and (b) ^{13}C NMR (100 MHz, CDCl_3) spectrum of **NAI-ANQ-NAI (DT)**
4. Figure S4. Solubility of **NAI-ANQ-NAIs** (0.5wt %) in chlorobenzene at room temperature
5. Figure S5. Solubility of **NAI-ANQ-NAIs** (0.5wt %) in chlorobenzene at 120 °C
6. Figure S6. Film quality of **NAI-ANQ-NAI** after spin-coating at 1000 rpm for 60 s
7. Figure S7. Transfer (a), output (b) characteristics and (c) gate-field dependent mobility of BGTC OFETs based on **NAI-ANQ-NAI (BO)** at annealing temperature of 140 °C
8. Figure S8. Transfer (a), output (b) characteristics and (c) gate-field dependent mobility of BGTC OFETs based on **NAI-ANQ-NAI (BO)** at annealing temperature of 160 °C
9. Figure S9. Transfer (a), output (b) characteristics and (c) gate-field dependent mobility of BGTC OFETs based on **NAI-ANQ-NAI (BO)** at annealing temperature of 180 °C
10. Figure S10. Transfer (a), output (b) characteristics and (c) gate-field dependent mobility of BGTC OFETs based on **NAI-ANQ-NAI (HD)** at annealing temperature of 140 °C
11. Figure S11. Transfer (a), output (b) characteristics and (c) gate-field dependent mobility of BGTC OFETs based on **NAI-ANQ-NAI (HD)** at annealing temperature of 160 °C
12. Figure S12. Transfer (a), output (b) characteristics and (c) gate-field dependent mobility of BGTC OFETs based on **NAI-ANQ-NAI (HD)** at annealing temperature of 180 °C
13. Figure S13. Transfer (a), output (b) characteristics and (c) gate-field dependent mobility of BGTC OFETs based on **NAI-ANQ-NAI (DT)** at annealing temperature of 140 °C
14. Figure S14. Transfer (a), output (b) characteristics and (c) gate-field dependent mobility of BGTC OFETs based on **NAI-ANQ-NAI (DT)** at annealing temperature of 160 °C
15. Figure S15. Transfer (a), output (b) characteristics and (c) gate-field dependent mobility of BGTC OFETs based on **NAI-ANQ-NAI (DT)** at annealing temperature of 180 °C
16. Figure S16. Transfer (left) characteristics and (right) gate-field dependent mobility of BGTC OFETs based on **NAI-ANQ-NAI (BO)** at annealing temperature of 240 °C.

17. Figure S17. Transfer (left) characteristics and (right) gate-field dependent mobility of BGTC OFETs based on **NAI-ANQ-NAI (HD)** at annealing temperature of 240 °C.
18. Figure S18. Transfer (left) characteristics and (right) gate-field dependent mobility of BGTC OFETs based on **NAI-ANQ-NAI (DT)** at annealing temperature of 240 °C.
19. Figure S19. AFM images ($5\mu \times 5\mu$) of thin films of **NAI-ANQ-NAI (BO)**, **NAI-ANQ-NAI (HD)** and **NAI-ANQ-NAI (DT)** at annealing temperature of 240 °C.
20. Table S1. Electron-transport properties of **NAI-ANQ-NAI (BO)** compounds based OFET devices annealed at 140 °C
21. Table S2. Electron-transport properties of **NAI-ANQ-NAI (BO)** compounds based OFET devices annealed at 160 °C
22. Table S3. Electron-transport properties of **NAI-ANQ-NAI (BO)** compounds based OFET devices annealed at 180 °C
23. Table S4. Electron-transport properties of **NAI-ANQ-NAI (HD)** compounds based OFET devices annealed at 140 °C
24. Table S5. Electron-transport properties of **NAI-ANQ-NAI (HD)** compounds based OFET devices annealed at 160 °C
25. Table S6. Electron-transport properties of **NAI-ANQ-NAI (HD)** compounds based OFET devices annealed at 180 °C
26. Table S7. Electron-transport properties of **NAI-ANQ-NAI (DT)** compounds based OFET devices annealed at 140 °C
27. Table S8. Electron-transport properties of **NAI-ANQ-NAI (DT)** compounds based OFET devices annealed at 160 °C
28. Table S9. Electron-transport properties of **NAI-ANQ-NAI (DT)** compounds based OFET devices annealed at 180 °C
29. Table S10. Electron-transport properties of **NAI-ANQ-NAI (BO)** compounds based OFET devices annealed at 200 °C
30. Table S11. Electron-transport properties of **NAI-ANQ-NAI (HD)** compounds based OFET devices annealed at 200 °C
31. Table S12. Electron-transport properties of **NAI-ANQ-NAI (DT)** compounds based OFET devices annealed at 200 °C

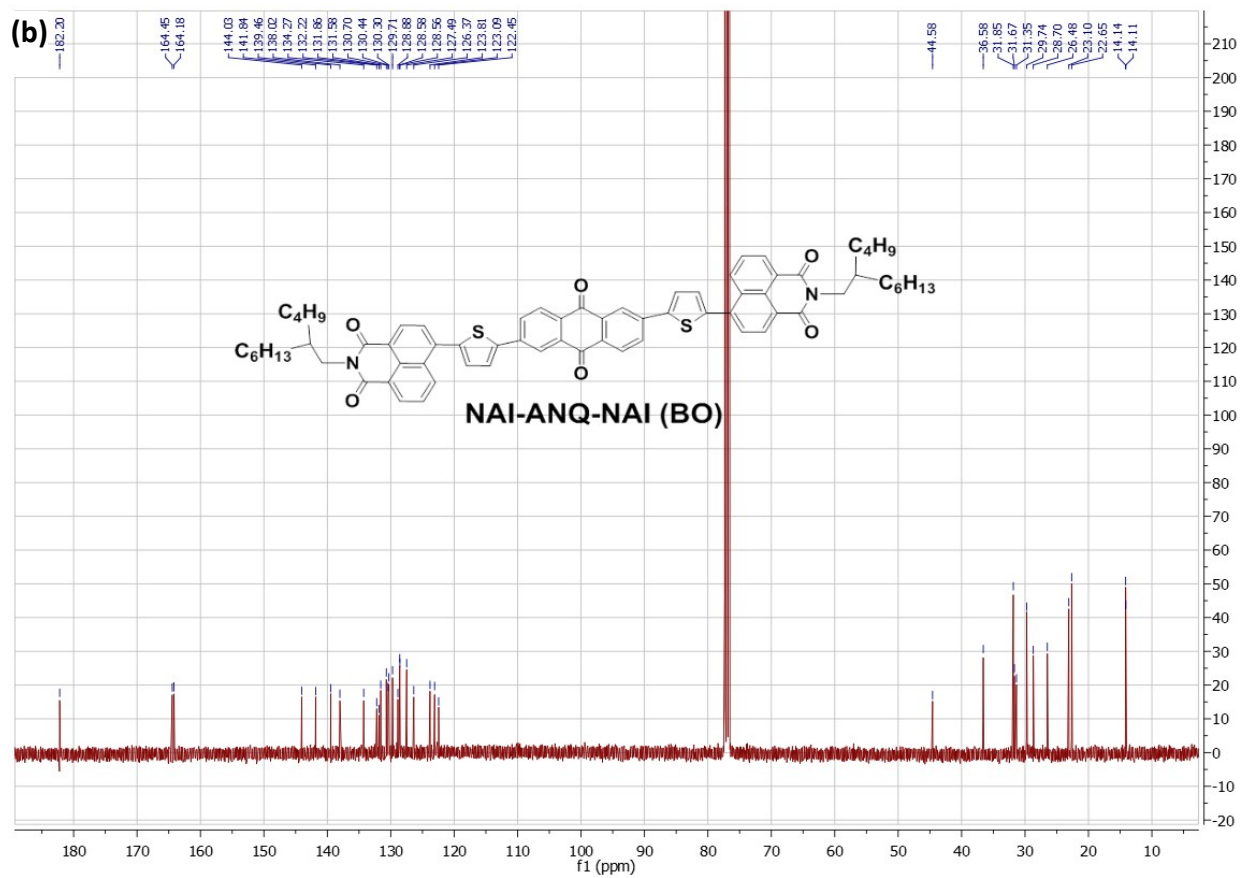
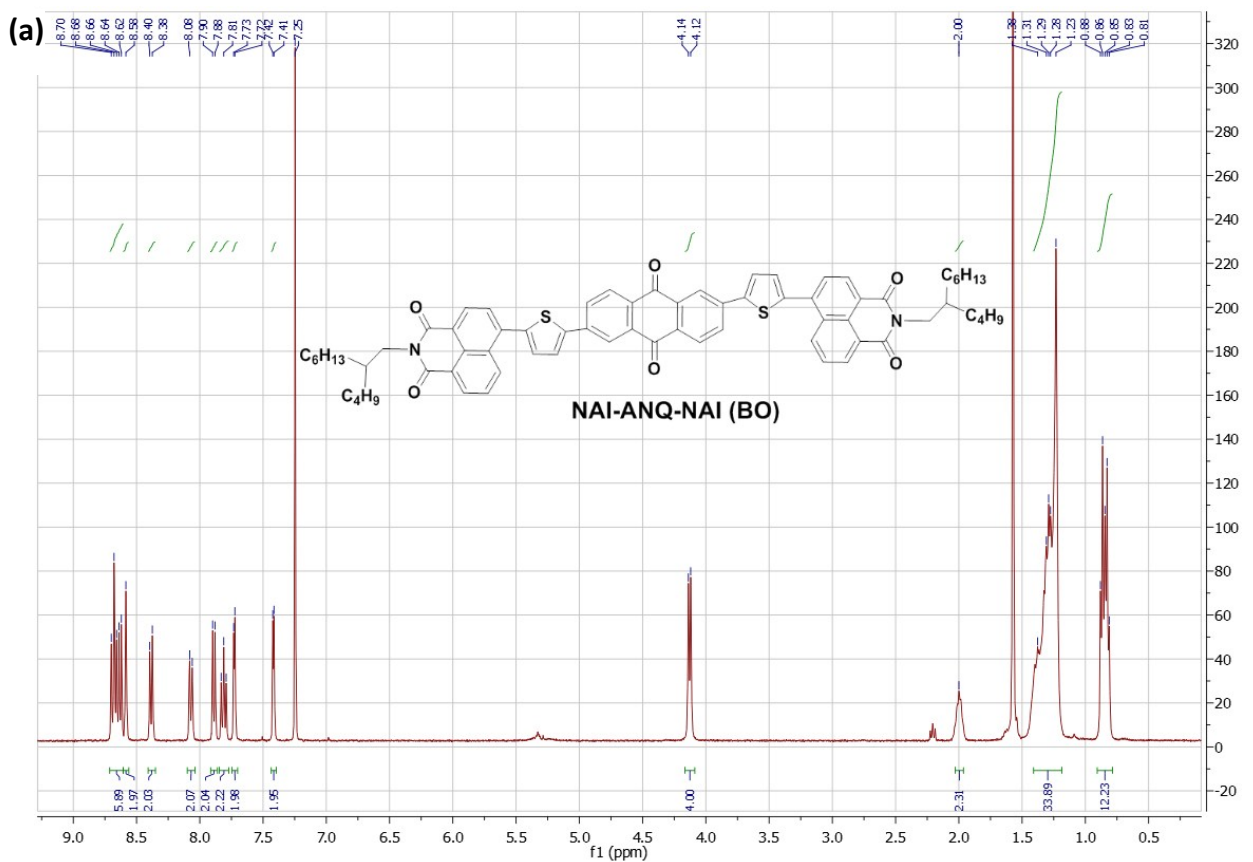


Figure S1. (a) ^1H NMR (400 MHz, CDCl_3) spectrum and (b) ^{13}C NMR (100 MHz, CDCl_3) spectrum of NAI-ANQ-NAI (BO)

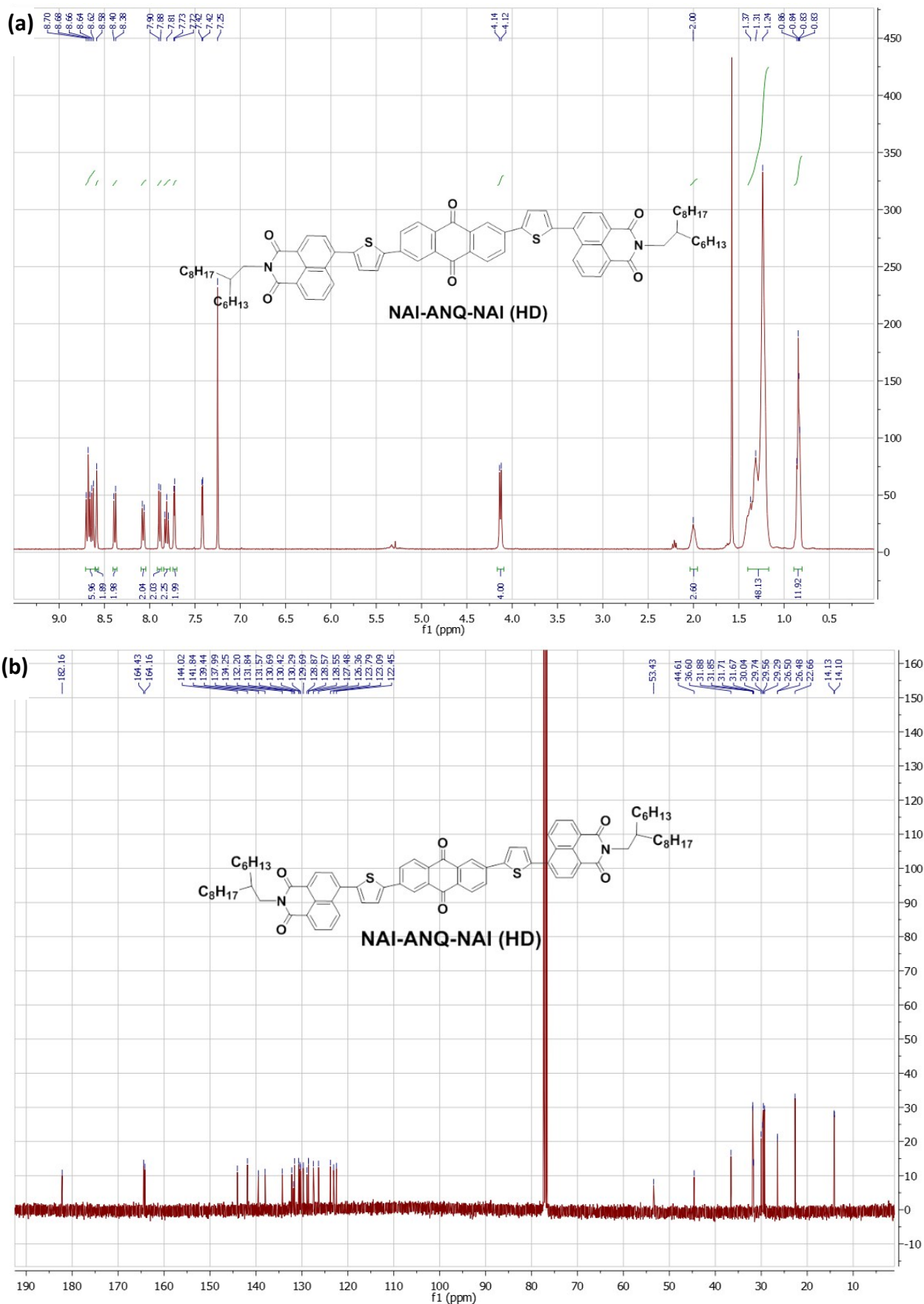


Figure S2. (a) ^1H NMR (400 MHz, CDCl_3) spectrum and (b) ^{13}C NMR (100 MHz, CDCl_3) spectrum of NAI-ANQ-NAI (HD)

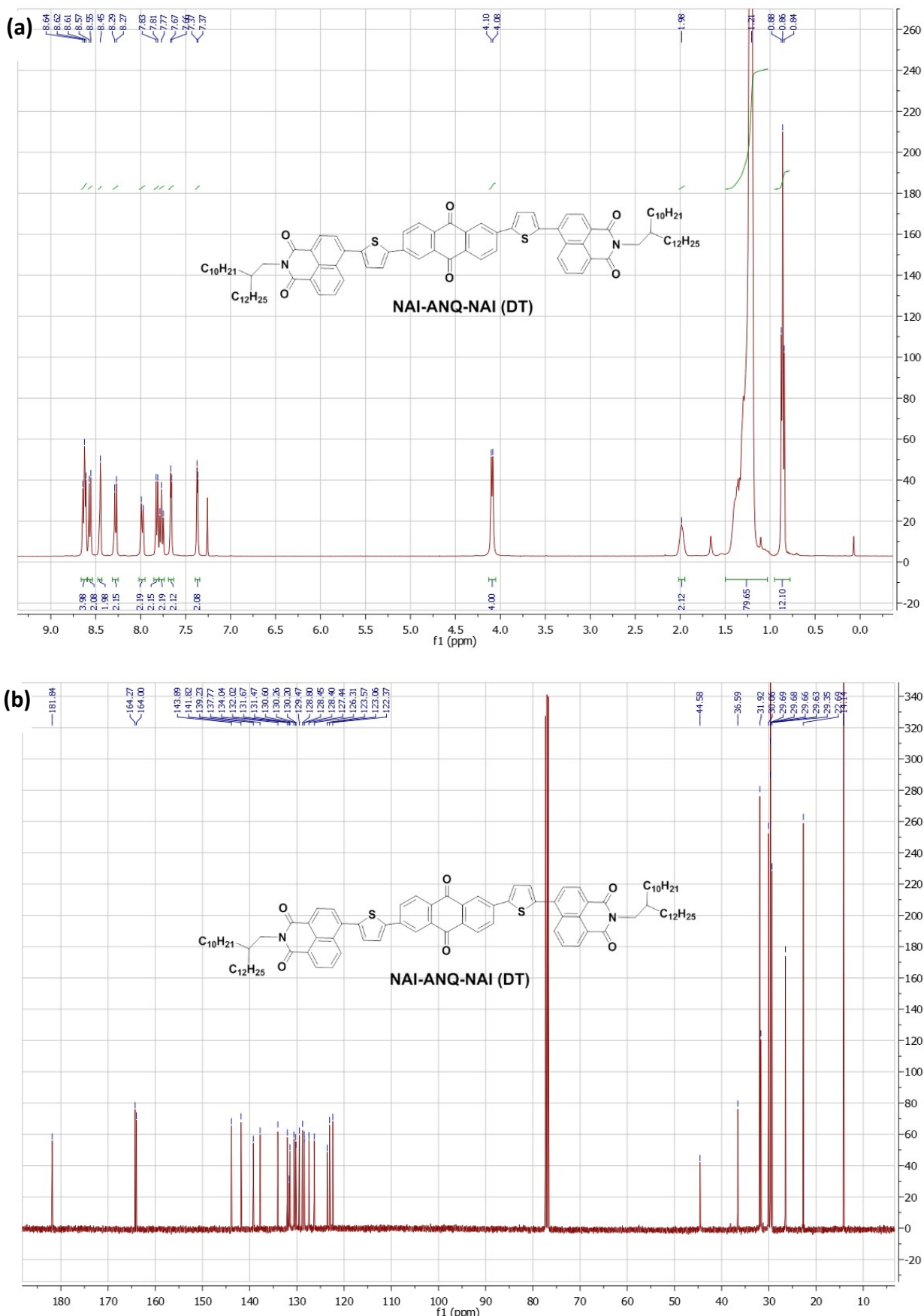


Figure S3. (a) ^1H NMR (400 MHz, CDCl_3) spectrum and (b) ^{13}C NMR (100 MHz, CDCl_3) spectrum of **NAI-ANQ-NAI (DT)**

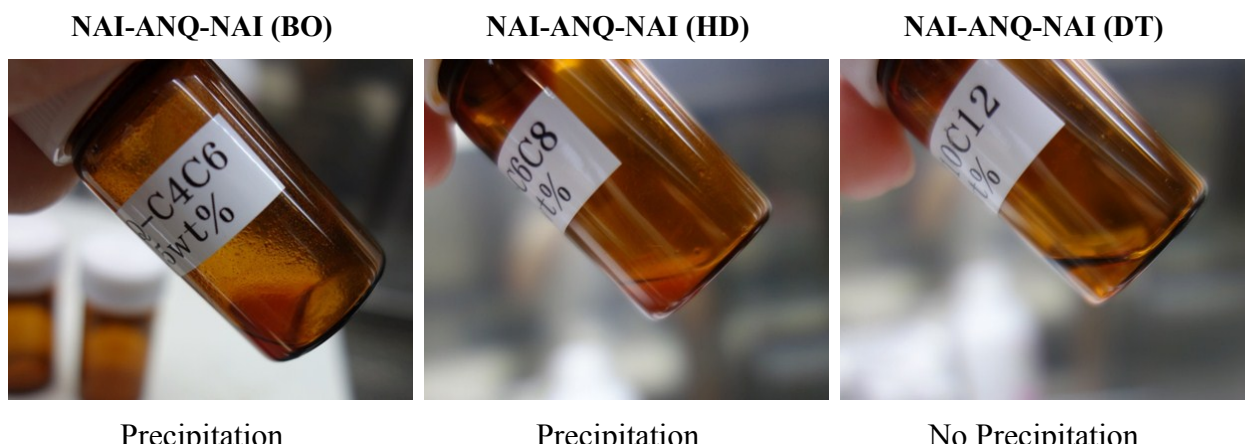


Figure S4. Solubility of **NAI-ANQ-NAIs** (0.5wt %) in chlorobenzene at room temperature

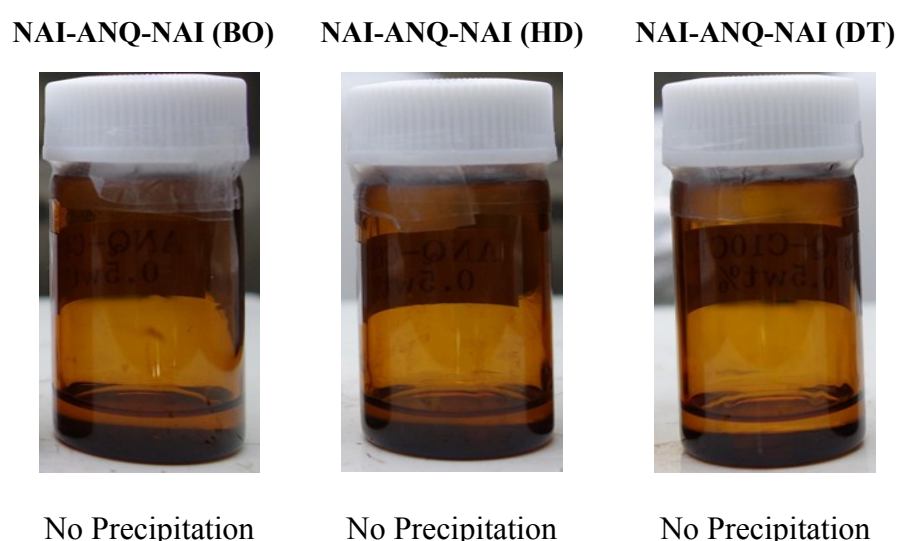


Figure S5. Solubility of **NAI-ANQ-NAIs** (0.5wt %) in chlorobenzene at 120 °C



Figure S6. Film quality of **NAI-ANQ-NAI** after spin-coating at 1000 rpm for 60 s

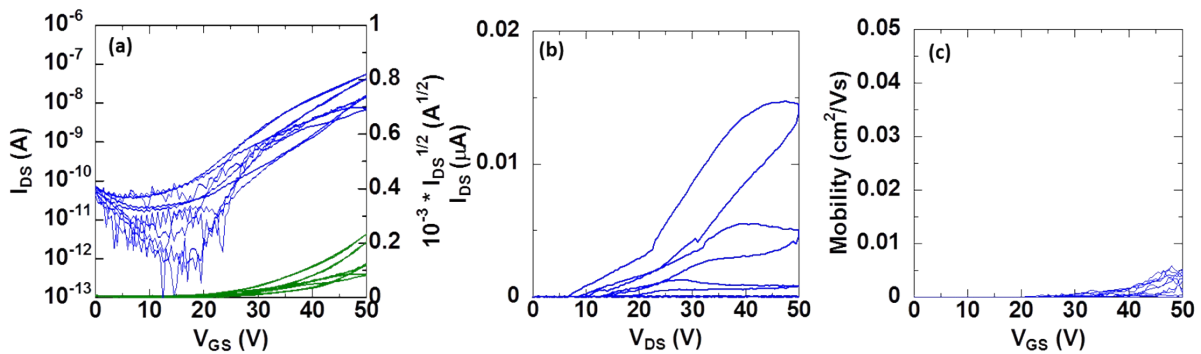


Figure S7. Transfer (a), output (b) characteristics and (c) gate-field dependent mobility of BGTC OFETs based on **NAI-ANQ-NAI (BO)** at annealing temperature of 140 °C

Table S1. Electron-transport properties of **NAI-ANQ-NAI (BO)** compounds based OFET devices annealed at 140 °C

Device	Mobility ($\text{cm}^2 \cdot \text{v}^{-1} \text{s}^{-1}$)	$I_{\text{on}} / I_{\text{off}}$	$V_{\text{TH}} (\text{V})$
1	3.45×10^{-4}	4.68×10^3	33.02
2	2.57×10^{-3}	6.44×10^4	40.61
3	1.47×10^{-3}	2.12×10^5	38.44
4	3.53×10^{-3}	1.95×10^4	35.40
5	3.94×10^{-3}	3.68×10^5	38.13
Avg	2.37×10^{-3}	1.34×10^5	37.1

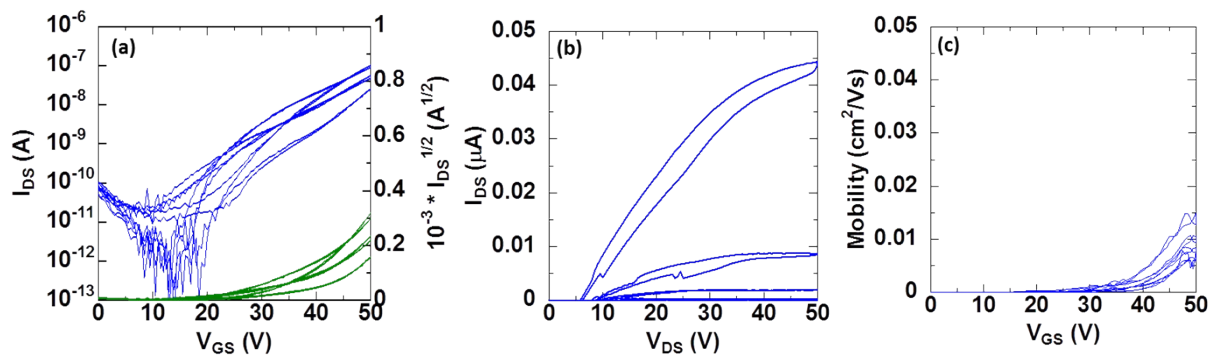


Figure S8. Transfer (a), output (b) characteristics and (c) gate-field dependent mobility of BGTC OFETs based on **NAI-ANQ-NAI (BO)** at annealing temperature of 160 °C

Table S2. Electron-transport properties of **NAI-ANQ-NAI (BO)** compounds based OFET devices annealed at 160 °C

Device	Mobility ($\text{cm}^2 \cdot \text{v}^{-1} \text{s}^{-1}$)	$I_{\text{on}} / I_{\text{off}}$	$V_{\text{TH}} (\text{V})$
1	5.69×10^{-3}	3.33×10^5	38.44
2	5.21×10^{-3}	6.00×10^5	41.65
3	4.41×10^{-3}	1.29×10^5	37.96
4	7.13×10^{-3}	6.26×10^5	36.94
5	9.93×10^{-3}	4.21×10^6	38.37
Avg	6.47×10^{-3}	1.18×10^6	38.7

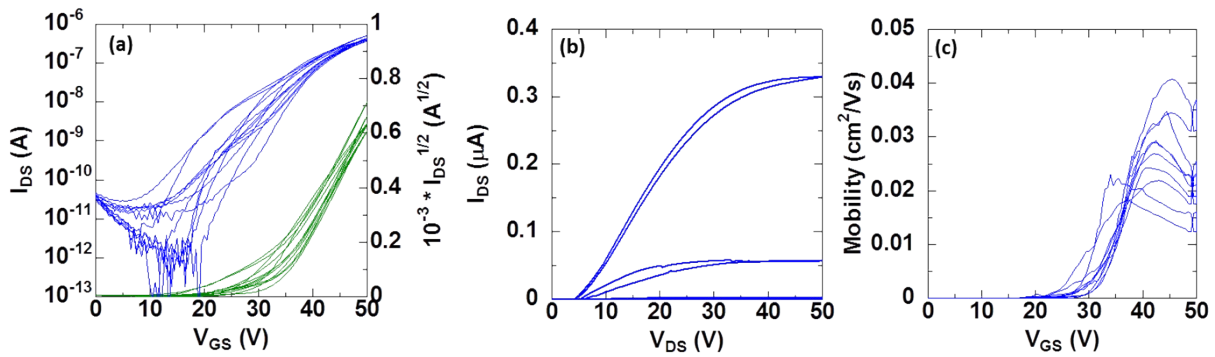


Figure S9. Transfer (a), output (b) characteristics and (c) gate-field dependent mobility of BGTC OFETs based on **NAI-ANQ-NAI (BO)** at annealing temperature of 180 °C

Table S3. Electron-transport properties of **NAI-ANQ-NAI (BO)** compounds based OFET devices annealed at 180 °C

Device	Mobility ($\text{cm}^2 \cdot \text{v}^{-1} \text{s}^{-1}$)	I_{on}/I_{off}	V_{TH} (V)
1	1.95×10^{-2}	1.16×10^6	33.69
2	1.53×10^{-2}	1.63×10^7	29.80
3	2.71×10^{-2}	1.78×10^7	34.96
4	2.27×10^{-2}	4.17×10^5	32.30
5	2.31×10^{-2}	1.27×10^7	34.59
Avg	2.16×10^{-2}	9.68×10^6	38.7

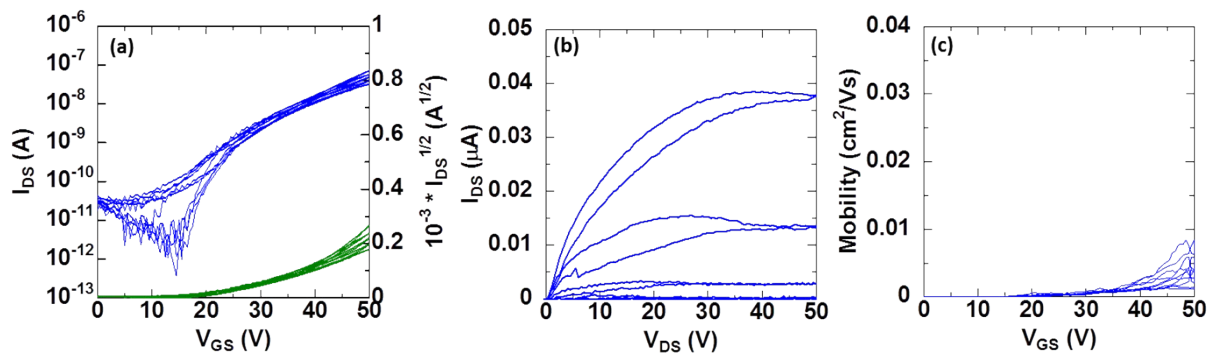


Figure S10. Transfer (a), output (b) characteristics and (c) gate-field dependent mobility of BGTC OFETs based on **NAI-ANQ-NAI (HD)** at annealing temperature of 140 °C

Table S4. Electron-transport properties of **NAI-ANQ-NAI (HD)** compounds based OFET devices annealed at 140 °C

Device	Mobility (cm ² .V ⁻¹ s ⁻¹)	I_{on}/I_{off}	V_{TH} (V)
1	5.59×10^{-3}	3.08×10^4	37.11
2	2.81×10^{-3}	1.63×10^4	33.23
3	2.92×10^{-3}	1.07×10^5	36.89
4	1.20×10^{-3}	3.00×10^4	29.96
5	3.95×10^{-3}	5.04×10^4	36.65
Avg	3.29×10^{-3}	4.69×10^4	34.77

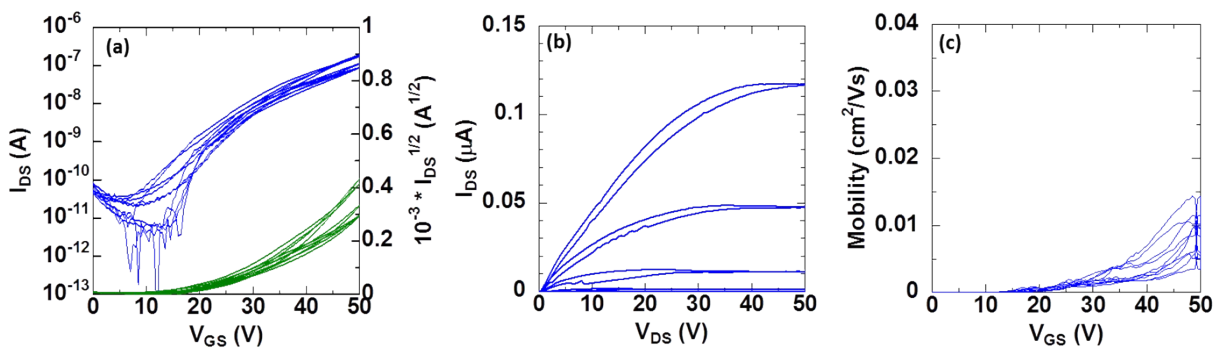


Figure S11. Transfer (a), output (b) characteristics and (c) gate-field dependent mobility of BGTC OFETs based on **NAI-ANQ-NAI (HD)** at annealing temperature of 160 °C

Table S5. Electron-transport properties of **NAI-ANQ-NAI (HD)** compounds based OFET devices annealed at 160 °C

Device	Mobility ($\text{cm}^2 \cdot \text{v}^{-1} \text{s}^{-1}$)	$I_{\text{on}} / I_{\text{off}}$	$V_{\text{TH}} (\text{V})$
1	3.91×10^{-3}	2.51×10^4	31.91
2	6.64×10^{-3}	1.79×10^4	36.18
3	9.60×10^{-3}	1.39×10^7	34.01
4	7.67×10^{-3}	1.79×10^4	32.34
5	6.48×10^{-3}	2.88×10^5	35.24
Avg	6.87×10^{-3}	2.86×10^6	33.9

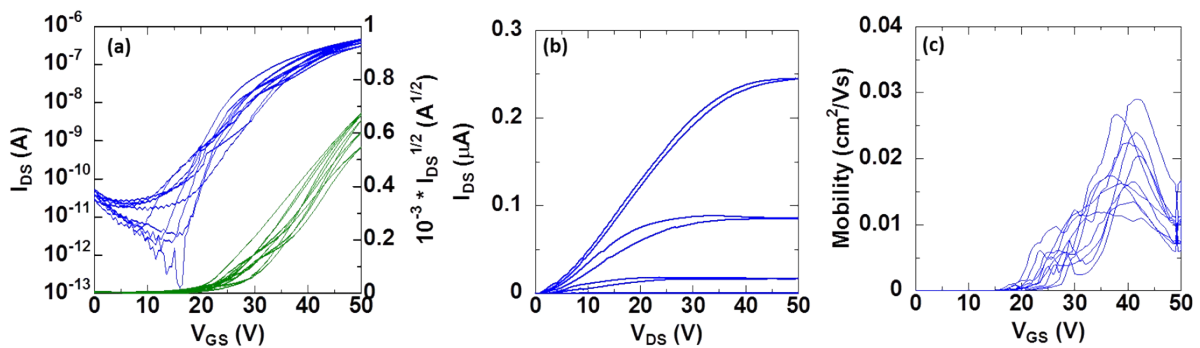


Figure S12. Transfer (a), output (b) characteristics and (c) gate-field dependent mobility of BGTC OFETs based on **NAl-ANQ-NAl (HD)** at annealing temperature of 180 °C

Table S6. Electron-transport properties of **NAl-ANQ-NAl (HD)** compounds based OFET devices annealed at 180 °C

Device	Mobility ($\text{cm}^2 \cdot \text{V}^{-1} \text{s}^{-1}$)	$I_{\text{on}}/I_{\text{off}}$	V_{TH} (V)
1	1.08×10^{-2}	1.88×10^5	25.60
2	1.60×10^{-2}	6.67×10^5	31.07
3	1.78×10^{-2}	3.17×10^5	30.06
4	1.36×10^{-2}	2.23×10^5	31.02
5	1.93×10^{-2}	1.40×10^5	31.48
Avg	1.55×10^{-2}	7.57×10^5	29.9

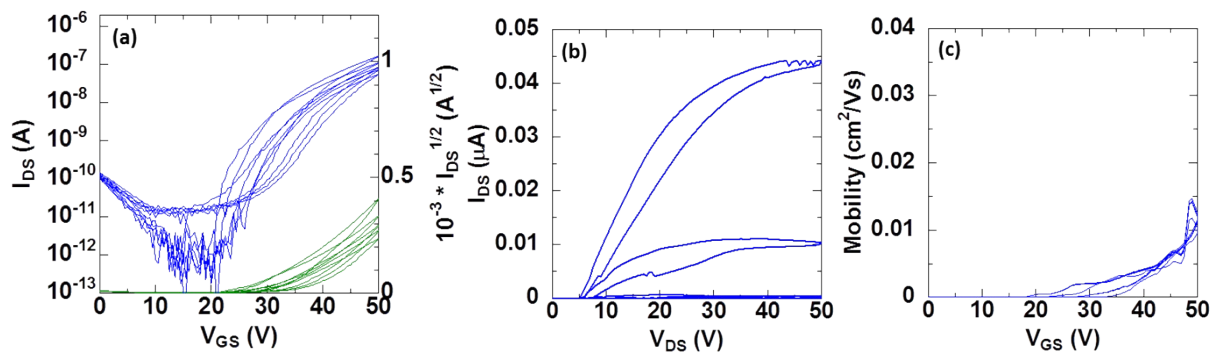


Figure S13. Transfer (a), output (b) characteristics and (c) gate-field dependent mobility of BGTC OFETs based on **NAI-ANQ-NAI (DT)** at annealing temperature of 140 °C

Table S7. Electron-transport properties of **NAI-ANQ-NAI (DT)** compounds based OFET devices annealed at 140 °C

Device	Mobility ($\text{cm}^2 \cdot \text{v}^{-1} \text{s}^{-1}$)	I_{on}/I_{off}	V_{TH} (V)
1	9.53×10^{-3}	6.15×10^5	38.70
2	7.87×10^{-3}	4.73×10^5	39.44
3	9.40×10^{-3}	9.27×10^5	39.25
4	9.80×10^{-3}	1.29×10^6	40.58
5	9.40×10^{-3}	3.24×10^5	40.26
Avg	9.20×10^{-3}	7.26×10^5	39.65

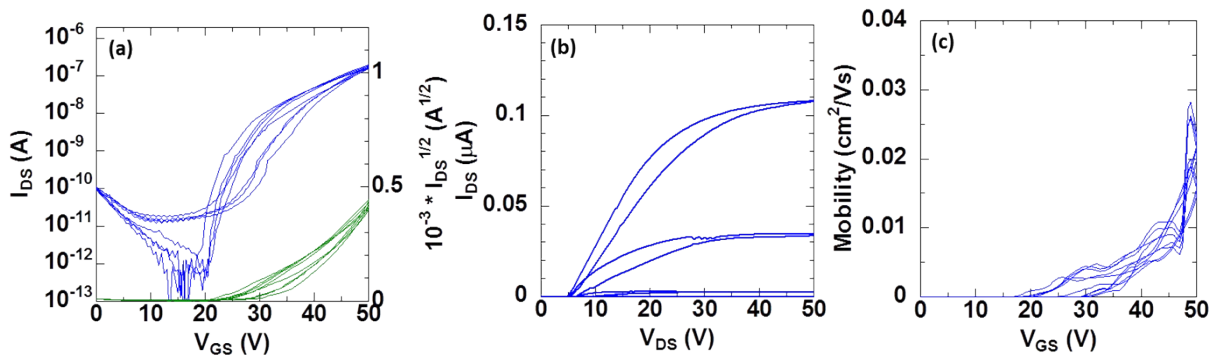


Figure S14. Transfer (a), output (b) characteristics and (c) gate-field dependent mobility of BGTC OFETs based on **NAI-ANQ-NAI (DT)** at annealing temperature of 160 °C

Table S8. Electron-transport properties of **NAI-ANQ-NAI (DT)** compounds based OFET devices annealed at 160 °C

Device	Mobility (cm ² .v ⁻¹ s ⁻¹)	I_{on}/I_{off}	V_{TH} (V)
1	1.33×10^{-2}	1.08×10^5	37.35
2	1.72×10^{-2}	4.93×10^7	38.37
3	1.88×10^{-2}	4.93×10^7	38.34
4	1.26×10^{-2}	3.18×10^6	38.39
5	1.75×10^{-2}	5.69×10^6	38.72
Avg	1.59×10^{-2}	2.15×10^7	38.23

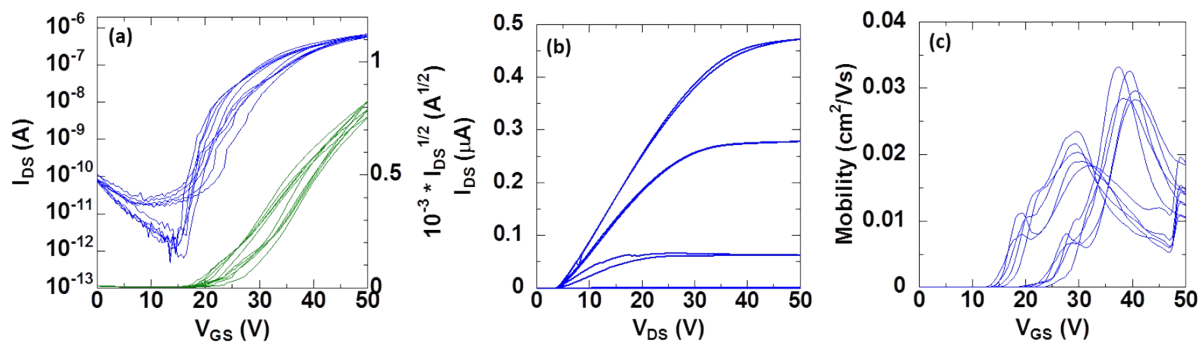


Figure S15. Transfer (a), output (b) characteristics and (c) gate-field dependent mobility of BGTC OFETs based on **NAI-ANQ-NAI (DT)** at annealing temperature of 180 °C

Table S9. Electron-transport properties of **NAI-ANQ-NAI (DT)** compounds based OFET devices annealed at 180 °C

Device	Mobility ($\text{cm}^2 \cdot \text{V}^{-1} \text{s}^{-1}$)	$I_{\text{on}} / I_{\text{off}}$	V_{TH} (V)
1	1.89×10^{-2}	7.65×10^5	26.90
2	2.21×10^{-2}	9.43×10^5	26.89
3	1.97×10^{-2}	7.28×10^5	27.02
4	1.89×10^{-2}	1.34×10^5	25.83
5	2.17×10^{-2}	9.01×10^5	28.20
Avg	2.03×10^{-2}	9.34×10^5	26.97

Table S10. Electron-transport properties of **NAI-ANQ-NAI (BO)** compounds based OFET devices annealed at 200 °C

Compound	Device	Electron Mobility (cm ² .V ⁻¹ s ⁻¹)	I_{on}/I_{off}	V _{th} (V)
NAI-ANQ-NAI (BO)	1	2.79 x 10⁻²	1.06 x 10⁷	24.27
	2	1.89 x 10 ⁻²	1.44 x 10 ⁷	24.62
	3	2.25 x 10 ⁻²	9.93 x 10 ⁴	25.06
	4	1.53 x 10 ⁻²	9.86 x 10 ⁴	23.58
	5	1.61 x 10 ⁻²	2.88 x 10 ⁵	23.01
	Avg	2.01 x 10 ⁻²	5.10 x 10 ⁶	24.1

Table S11. Electron-transport properties of **NAI-ANQ-NAI (HD)** compounds based OFET devices annealed at 200 °C

Compound	Device	Electron Mobility (cm ² .V ⁻¹ s ⁻¹)	I_{on}/I_{off}	V _{th} (V)
NAI-ANQ-NAI (HD)	1	1.32 x 10 ⁻²	1.09 x 10 ⁵	19.31
	2	2.09 x 10⁻²	2.39 x 10⁵	22.37
	3	1.73 x 10 ⁻²	1.45 x 10 ⁶	21.32
	4	1.39 x 10 ⁻²	3.21 x 10 ⁵	21.88
	5	2.05 x 10 ⁻²	2.45 x 10 ⁵	21.75
	Avg	1.71 x 10 ⁻²	4.73 x 10 ⁵	21.3

Table S12. Electron-transport properties of **NAI-ANQ-NAI (DT)** compounds based OFET devices annealed at 200 °C

Compound	Device	Electron Mobility (cm ² .V ⁻¹ s ⁻¹)	I_{on}/I_{off}	V _{th} (V)
NAI-ANQ- NAI (DT)	1	1.52 x 10 ⁻²	1.54 x 10 ⁵	17.03
	2	2.40 x 10⁻²	2.56 x 10⁵	13.38
	3	8.40 x 10 ⁻³	1.02 x 10 ⁵	16.90
	4	1.41 x 10 ⁻²	2.26 x 10 ⁵	18.42
	5	2.27 x 10 ⁻²	3.65 x 10 ⁵	19.37
	Avg	1.69 x 10 ⁻²	2.28 x 10 ⁵	21.3

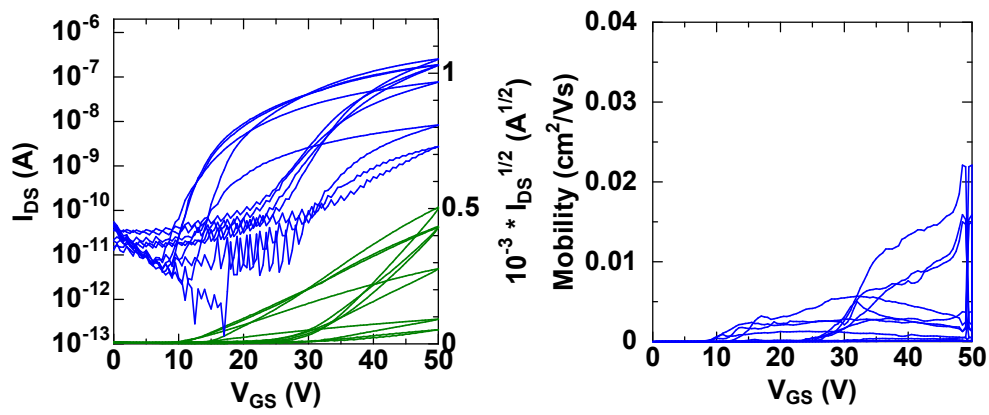


Figure S16. Transfer (left) characteristics and (right) gate-field dependent mobility of BGTC OFETs based on **NAI-ANQ-NAI (BO)** at annealing temperature of 240 °C.

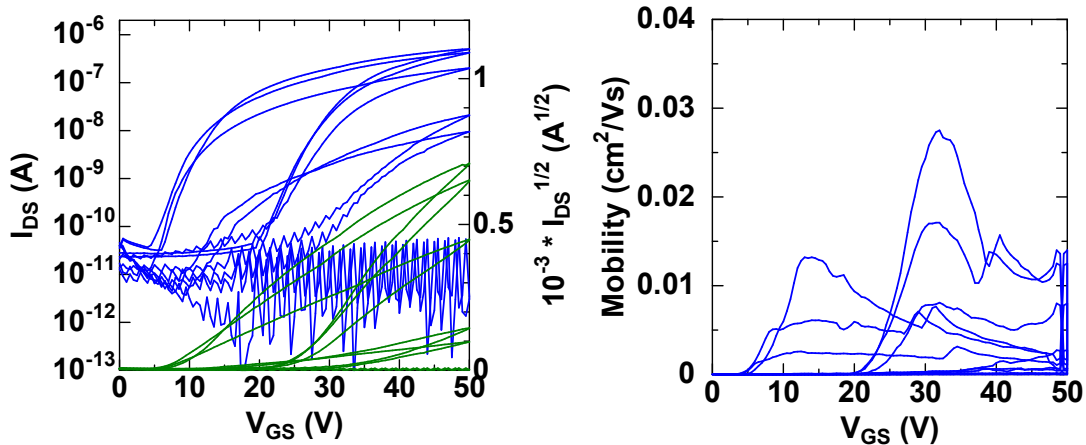


Figure S17. Transfer (left) characteristics and (right) gate-field dependent mobility of BGTC OFETs based on **NAI-ANQ-NAI (HD)** at annealing temperature of 240 °C.

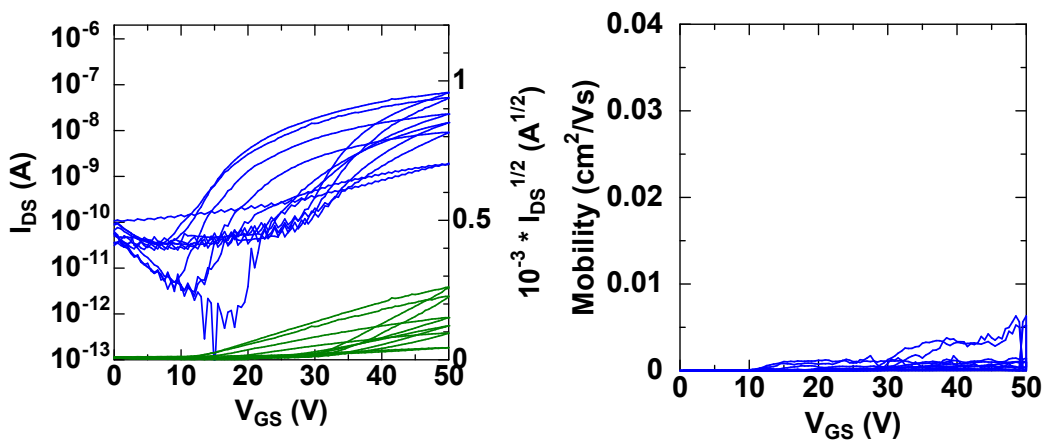


Figure S18. Transfer (left) characteristics and (right) gate-field dependent mobility of BGTC OFETs based on **NAI-ANQ-NAI (DT)** at annealing temperature of 240 °C.

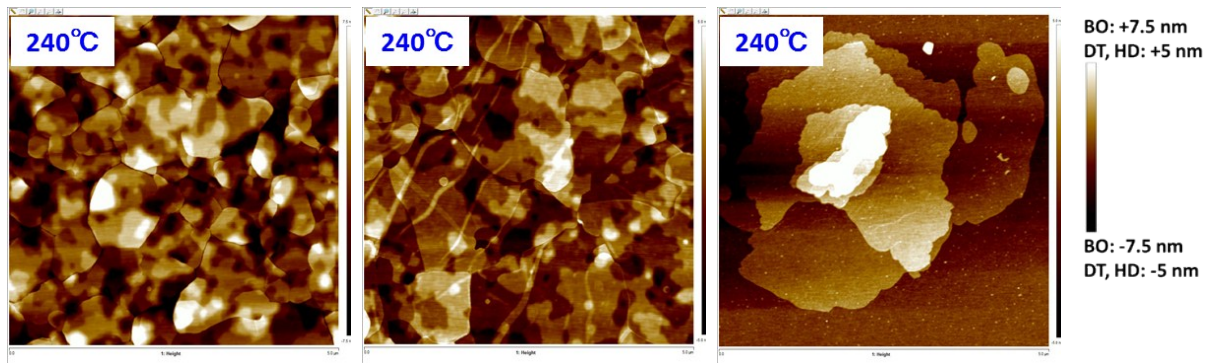


Figure S19. AFM images (5 μ x 5 μ) of thin films of **NAI-ANQ-NAI (BO)**, **NAI-ANQ-NAI (HD)** and **NAI-ANQ-NAI (DT)** at annealing temperature of 240°C.